Damage identification technique by model enrichment for structural elastodynamic problems

Daniele Di Lorenzo, Sebastian Rodriguez, Laurent Champaney, Claudia Germoso, Marianne Beringhier, Francisco Chinesta Soria

Damage identification technique by model enrichment for structural elastodynamic problems

D. Di Lorenzo [a,b,*], S. Rodriguez [b], V. Champaney [b], C. Germoso [c], M. Beringhier [d], F. Chinesta [a,b]

[a] ESI Group, 3bis, Rue Saarinen CEDEX, Rungis, 94528, France
[b] PIMM Lab, ENSAM Institute of Technology, 151 Boulevard de l'Hôpital, Paris, 75013, France
[c] Instituto Tecnológico de Santo Domingo (INTEC), Av. Los Próceres, Jardines del Norte, Santo Domingo, República Dominicana
[d] Institut PPRIME, ISAE-ENSMA, Téléport 2, 1 Av. Clément Ader, Chasseneuil-du-Poitou, 86360, France

ARTICLE INFO

Keywords:
Structural dynamics
Model-order reduction techniques
Structural Health Monitoring
Localized damage
Model enrichment
Sparse identification

ABSTRACT

Structural Health Monitoring (SHM) techniques are key to monitor the health state of engineering structures, where damage type, location and severity are to be estimated by applying sophisticated techniques to signals measured by sensors. However, very localized damage detection algorithms applied to dynamics problems when dealing with rigid structures at low-frequency range remains still a big challenge. The last due to the low influence of very localized damage on the overall response of the structure (Saint-Venant principle). In this context, in the present work, we propose a methodology for locally correcting the models from collected data for elastodynamics problems at low-frequency range which is able to predict very localized damage. The proposed technique consists in enriching the structural model in a sparse way and solving the identification problem in the frequency domain, where the influence of damage over a large frequency band is exploited to improve the prediction of the damage location. The advantages and potential of the proposed technique are illustrated for the damage detection in a plate problem, demonstrating the advantages of the method in detecting very localized damage. The proposed technique is limited to a methodological description, and further developments should be considered to approach its applicability in an industrial scenario.

1. Introduction

Over the last decades, many techniques have been developed in the field of Structural Health Monitoring in order to address damage detection [1]. Those techniques are non-destructive techniques and in particular, it is possible to classify the general used methods in frequency and time domains. Frequency domain techniques [2–5] are based on modal analysis, and this can represent a great advantage when a range of frequencies to be analyzed is known a priori. Time domain techniques on the other hand, are based on the study of vibration features and signal processing techniques [6–11], additionally, one finds techniques based on Matching Pursuit (MP) [12–15] applied to ultrasonic Lamb Waves (LW) emitted and received by piezoelectric elements (PZT) [16–19]. In those techniques damage detection is achieved by looking at how the features of the MP decomposition applied to signals coming from a healthy structure change with respect to a damaged one. Also one finds spatial techniques based on wavelet analysis applied to modal basis [20–24].

However, dedicated techniques for the correct monitoring of very stiff structures when dealing with very localized damage in low-frequency range still remains a major challenge. This last, is principally due to the fact that the perturbed effect due to the existence of damage remains very localized, being very difficult the detection of damage location from the measurement of few sensors far from the damaged zone, which is known as the Saint-Venant principles in elastostatics. For this reason, in our previous work [25], a model correction technique was proposed in order to enrich a model and at the same time produce damage identification. However, its applicability was limited to quasi-static problems.

Here, this technique is extended from quasi-static analysis to the dynamic one, where richer information is available in the temporal and frequency domain for the accurate enrichment and damage detection. The proposed technique consists of finding a model correction based on

* Corresponding author.
E-mail address: daniele.di_lorenzo@ensam.eu (D. Di Lorenzo).

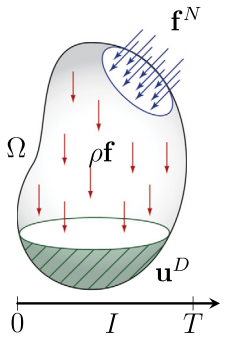

Fig. 1. The mechanical domain under study.

the knowledge of data from a few sensors, these sensors measure the time evolution of the displacements (or strain) of a real structure. The model uses this information in the frequency domain of the measured data to locally enrich a nominal model. Damage detection is enhanced due to the enriched information on how damage influences the frequency spectrum response of the nominal structure. This correction is later used to identify the location and severity of the damage.

The present paper is structured as follows: Section 2 presents the reference problem, Section 3 presents the technique for local enrichment of a model and its use in damage detection. Later Section 4 presents different numerical examples showing the application of the proposed technique for the identification of damage. Finally, Section 5 provides conclusions and perspectives.

2. Reference problem

Let us consider the structure of Fig. 1 occupying the spatial domain $\Omega \subset \mathbb{R}^d$ with $d \in \{1,2,3\}$, on a time domain $I = [0,T]$ and with constant boundary $\partial\Omega = \partial_N\Omega \oplus \partial_D\Omega$ over time, where $\partial_N\Omega$ and $\partial_D\Omega$ are the boundaries related to the imposed Neumann and Dirichlet conditions respectively. This structure is submitted to: surface forces $\mathbf{f}^N$ on $\partial_N\Omega \times I$ (Neumann boundary conditions), imposed displacements $\mathbf{u}^D$ on $\partial_D\Omega \times I$ (Dirichlet boundary condition) and volumetric forces $\rho\mathbf{f}$ on $\Omega \times I$. In order to find the displacement field $\mathbf{u}(\mathbf{x},t)$ of the structure we need to solve:

$$\begin{cases} \mathrm{div}(\boldsymbol{\sigma}) + \rho\mathbf{f} = \rho\ddot{\mathbf{u}} & \text{in } \Omega \times I \\ \boldsymbol{\sigma}\cdot\mathbf{n} = \mathbf{f}^N & \text{on } \partial_N\Omega \times I \\ \mathbf{u} = \mathbf{u}^D & \text{on } \partial_D\Omega \times I \\ \mathbf{u}(\mathbf{x},0) = \boldsymbol{\psi}(\mathbf{x}) & \text{in } \Omega \\ \dot{\mathbf{u}}(\mathbf{x},0) = \boldsymbol{\gamma}(\mathbf{x}) & \text{in } \Omega \\ \boldsymbol{\varepsilon} = \frac{\nabla\mathbf{u} + \nabla\mathbf{u}^T}{2} \end{cases} \tag{1}$$

with ∇ the gradient operator, $\boldsymbol{\sigma}$ the stress field and $\boldsymbol{\varepsilon}$ the strain. For what follows we assume that the stress tensor is composed by two component:

$$\boldsymbol{\sigma} = \boldsymbol{\sigma}_v + \boldsymbol{\sigma}_e, \tag{2}$$

where $\boldsymbol{\sigma}_e$ represent the elastic contribution and $\boldsymbol{\sigma}_v$ the viscosity one. For the elastic part Hooke's constitutive law is considered so:

$$\boldsymbol{\sigma}_e = \mathsf{C} : \boldsymbol{\varepsilon}, \tag{3}$$

with C the Hooke's tensor, while the viscous term is given by:

$$\boldsymbol{\sigma}_v = \mathsf{D} : \dot{\boldsymbol{\varepsilon}}, \tag{4}$$

where D corresponds to the viscosity tensor. This tensor is chosen in order to obtain a specific damping behavior and, as will be seen later, we will simply consider proportional damping. In addition since in this paper we are dealing with damage detection, only isotropic damage behavior will be considered and so in case the equation (3) becomes:

$$\boldsymbol{\sigma}_e = (1-d)\mathsf{C} : \boldsymbol{\varepsilon}, \tag{5}$$

with $d \in [0,1]$ corresponding to the severity of the damage.

3. Local correction procedure

The continuous formulation of equation (1) is solved by discretizing it in the spatial domain, this is classically done employing the FEM method [26], where the following system of equations is obtained:

$$\mathbf{M}\ddot{\mathbf{u}} + \mathbf{D}\dot{\mathbf{u}} + \mathbf{K}\mathbf{u} = \mathbf{f}, \tag{6}$$

where $\mathbf{M}$, $\mathbf{D}$, $\mathbf{K}$ represent respectively the mass, damping and stiffness matrix and $\ddot{\mathbf{u}}, \dot{\mathbf{u}}, \mathbf{u}$ are the acceleration the velocity and the displacement field respectively. However, if we assume that both the nominal model and the displacement field require correction, we should introduce corrections for all matrices as well as the displacement, velocity, and acceleration fields into the formulation (6), resulting in:

$$(\mathbf{M}+\Delta\mathbf{M})(\ddot{\mathbf{u}}+\Delta\ddot{\mathbf{u}}) + (\mathbf{D}+\Delta\mathbf{D})(\dot{\mathbf{u}}+\Delta\dot{\mathbf{u}}) + (\mathbf{K}+\Delta\mathbf{K})(\mathbf{u}+\Delta\mathbf{u}) = \mathbf{f}. \tag{7}$$

A simpler approach is to apply the Fourier transform to (6) before considering the need for any correction:

$$(-\omega^2\mathbf{M} + i\omega\mathbf{D} + \mathbf{K})\hat{\mathbf{u}} = \hat{\mathbf{f}}, \tag{8}$$

where the symbol $\hat{\bullet}$ represents the Fourier transform of $\bullet$. Introducing then a correction, equation (8) becomes:

$$[-\omega^2(\mathbf{M}+\Delta\mathbf{M}) + i\omega(\mathbf{D}+\Delta\mathbf{D}) + (\mathbf{K}+\Delta\mathbf{K})](\hat{\mathbf{u}}+\Delta\hat{\mathbf{u}}) = \hat{\mathbf{f}}. \tag{9}$$

By assuming a proportional damping representation:

$$\mathbf{D} = \alpha\mathbf{M} + \beta\mathbf{K}, \tag{10}$$

where α and β are positive real number lower or equal to one, we have that the correction of the damping becomes:

$$\Delta\mathbf{D} = \alpha\Delta\mathbf{M} + \beta\Delta\mathbf{K}. \tag{11}$$

We can thus rewrite equation (9) as:

$$\{-\omega^2(\mathbf{M}+\Delta\mathbf{M}) + i\omega[\alpha(\mathbf{M}+\Delta\mathbf{M}) + \beta(\mathbf{K}+\Delta\mathbf{K})] + (\mathbf{K}+\Delta\mathbf{K})\}(\hat{\mathbf{u}}+\Delta\hat{\mathbf{u}}) = \hat{\mathbf{f}}. \tag{12}$$

The linearized problem becomes:

$$(-\omega^2 + i\omega\alpha)\mathbf{M}\Delta\hat{\mathbf{u}} + (1 + i\omega\beta)(\mathbf{K}\Delta\hat{\mathbf{u}} + \Delta\mathbf{K}\,\hat{\mathbf{u}}) = 0 \tag{13}$$

where we assumed $\Delta\mathbf{M} = 0$, under the hypothesis that damage to the structure does not affect its mass.

In (13) two unknowns should be determined, the correction of the stiffness matrix and displacement $\Delta\mathbf{K}$ and $\Delta\hat{\mathbf{u}}$ respectively. For a given $\Delta\mathbf{K}$ the correction of displacement can be computed through classic FEM, however, given a displacement correction, the determination of $\Delta\mathbf{K}$ is not direct. In this, sense, in order to solve the correction of the stiffness matrix, one approach consists in adopting a parameterization for $\Delta\mathbf{K}$. A possible approximation is expressed as follows:

$$\Delta\mathbf{K} = \sum_{i=1}^{N_e} a_i\mathbf{K}_i^e \tag{14}$$

where N_e is the number of elements in the mesh used to discretize the domain Ω, i.e., $\Omega = \cup_{i=1}^{N_e}\Omega_i$ and where $\mathbf{K}_i^e$ is the nominal stiffness matrix with respect to element Ω_i. The expression (14), with $a_i < 0$, represents a simple approximation method of diminishing the contribution of element Ω_i to the structure's stiffness matrix $\mathbf{K}$. For elements located in the undamaged region there is no need for correction, and therefore

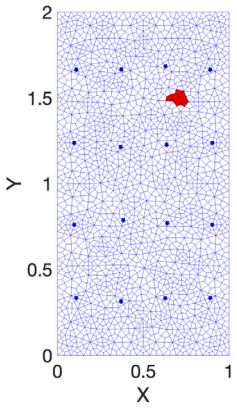

(a) Damaged region (red elements) in the plate and location of the 16 sensors (blue nodes).

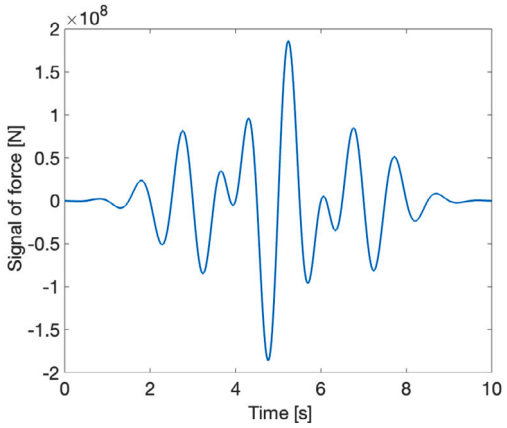

(b) Magnitude of the load over time ($f(t)$) applied to the structure. The load has the same component in the x and y directions.

Fig. 2. Problem configuration plate.

the associated coefficients will vanish. Thus, it is expected that only the elements in the set $\mathcal{E}$ concerned by the elements covering the damaged area will have non zero values of the a-coefficients. Therefore, the minimization problem that enforces the expected sparsity of the a-coefficients is described as follows:

$$\begin{cases} \min\limits_{\{a_i\}_{i=1}^{N_e}} \sum\limits_{i=1}^{N_e} |a_i| \\ \text{subjected to: } (-\omega^2 + i\omega\alpha)\mathbf{M}\Delta\hat{\mathbf{u}}(\omega) + (1 + i\omega\beta)(\mathbf{K}\Delta\hat{\mathbf{u}}(\omega) + \Delta\mathbf{K}\,\hat{\mathbf{u}}(\omega)) = 0 \\ \;\&\; \hat{\mathbf{u}}(\omega)(\mathbf{x}_{sens}, \omega) + \Delta\hat{\mathbf{u}}(\mathbf{x}_{sens}, \omega) = \hat{\mathbf{u}}^m(\mathbf{x}_{sens}, \omega) \end{cases} \tag{15}$$

where $\hat{\mathbf{u}}^m(\omega)$ corresponds to the Fourier transform of the measured displacement data, $\hat{\mathbf{u}}(\mathbf{x}_{sens}, \omega)$ and $\Delta\hat{\mathbf{u}}(\mathbf{x}_{sens}, \omega)$ to the nominal displacement and its respectively correction on sensor locations $\mathbf{x}_{sens}$ respectively.

Note from the expression (15) that there are as many expressions as there are different measures of the displacement response at different frequencies ω and for each of these frequencies, the numerical solution of the nominal state of the structure must be calculated. The fact of having as many expressions to verify as experimental frequency measurements is of utmost importance, since this generates a large amount of data to generate an effective and accurate detection of damage, which does not happen in the case of quasi-statics, where only one experimental measurement is available to generate a detection of damage. Once all the variables of problem (15) defined, this problem is solved using convex optimization algorithms [27], implemented using the Matlab library CVX [28].

4. Case study analysis

4.1. Plate

In this section, we applied the proposed methodology to a plate of dimensions $d_1 = 1$ $[m]$, $d_2 = 2$ $[m]$. This plate is fully clamped on its bottom boundary, free on the other boundaries and subjected to a load varying in time on its left side upper corner. The applied force (Fig. 2b) is defined as a combination of sinusoids at different frequencies:

$$f(t) = 2 \cdot 10^8 \cdot \left(2\pi^2 \frac{(t-5)^2}{25} - 1\right) \cdot e^{\left(-\pi^2 \frac{(t-5)^2}{25} - 1\right)} \cdot sin(2\pi \cdot t), \tag{16}$$

in order to excite a wide spectrum of frequencies, which will be used to identify the location of the damage by solving (15). However due to computational burden only three frequencies have been chosen (2.95, 5.95, 11.95 Hz) to run the algorithm.

The plate is modeled under a plane stress condition and its behavior is assumed to be elastic, characterized by a Young's modulus of $E = 200$ GPa and a Poisson's coefficient of $\nu = 0.3$. This configuration corresponds to the nominal structural system, while the reference system is assumed to contain a damaged area. The plate is equipped with a finite element mesh, depicted in Fig. 2a, which serves as support for the approximation of various mechanical fields: displacement, strains and stresses. The elements located in the damaged region are highlighted in red in Fig. 2a. In this region, the Young's modulus is reduced to $E' = 0.2 \cdot E$, i.e. $d = 0.8$ as shown in (3). For the sake of simplicity, the locations of the sensors are assumed to coincide with some of the mesh nodes, particularly the ones marked in blue in Fig. 2a. Figs. 3 - 4 c (x and y components) of the damaged and undamaged structures for two different time steps (5.24 and 7.24 seconds). As we can see, since the damage is localized, the difference between the two structures is not significant. After solving the minimization problem, the elements that underwent the most significant corrections are visually highlighted in red in Fig. 5a, showcasing a successful identification of the damage (Fig. 5b). To further validate this methodology, we addressed a scenario where only one element is damaged (Fig. 6). Notably, in this case, the algorithm shows remarkable accuracy in pinpointing the location of the damage.

4.2. Plate with an hole

In order to show the validity of the presented method, another geometry is considered. In particular, let's consider a plate with a hole (Fig. 7a), with dimensions $d_1 = 2.5$ m, $d_2 = 4$ m, and a hole of radius $r = 0.25$ m. The same configuration (boundary conditions, material properties, and force location) described in Sec. 4.1 has also been used for this plate. However, for this case, a slightly different force (Fig. 7b) has been applied to the structure:

$$f(t) = -2 \cdot 10^8 \cdot \left(2\pi^2 \frac{(t-5)^2}{25} - 1\right) \cdot e^{\left(-\pi^2 \frac{(t-5)^2}{25} - 1\right)} \cdot sin(4\pi \cdot t). \tag{17}$$

As already mention in Sec. 4.1 due to computational burden only two frequencies have been chosen (19, 93 Hz) to run the algorithm (15). Fig. 8 compare the displacement field (x and y components) of the damaged and undamaged structures at 5.12 seconds. The result of the identification procedure is shown in Fig. 9. Also in this case, the algorithm identifies with good accuracy the location of the damage.

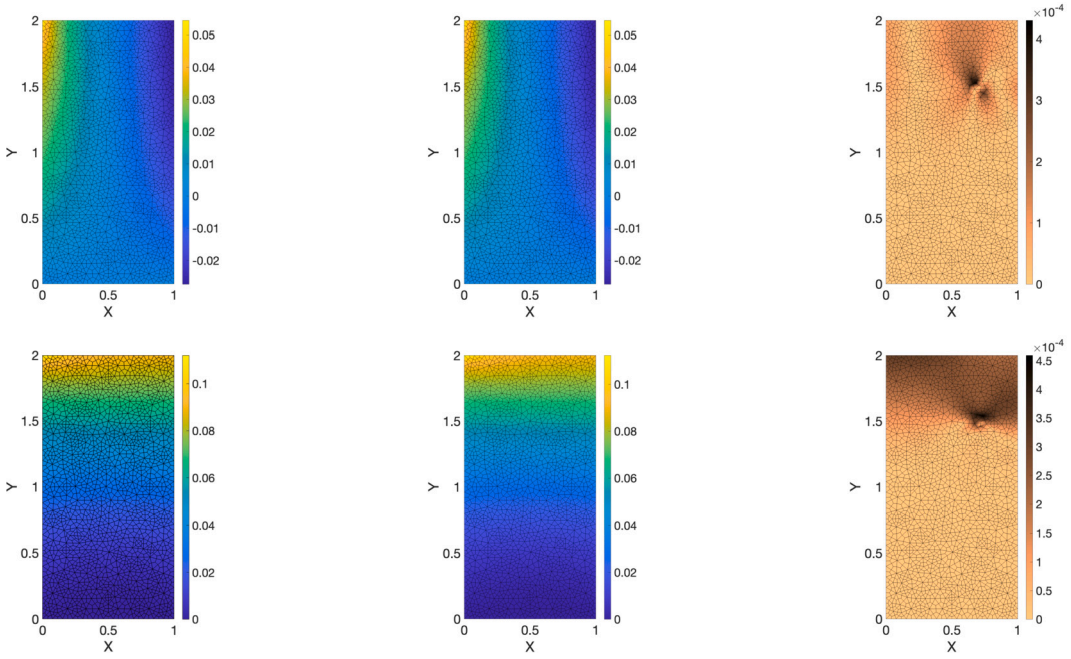

Fig. 3. x (**top**), y (**bottom**) components of the displacement field associated with the nominal solution (**left**); reference solution that takes into account the real damaged region (**middle**) and difference in absolute absolute between the two solutions (**right**) at time $t = 5.24$ s.

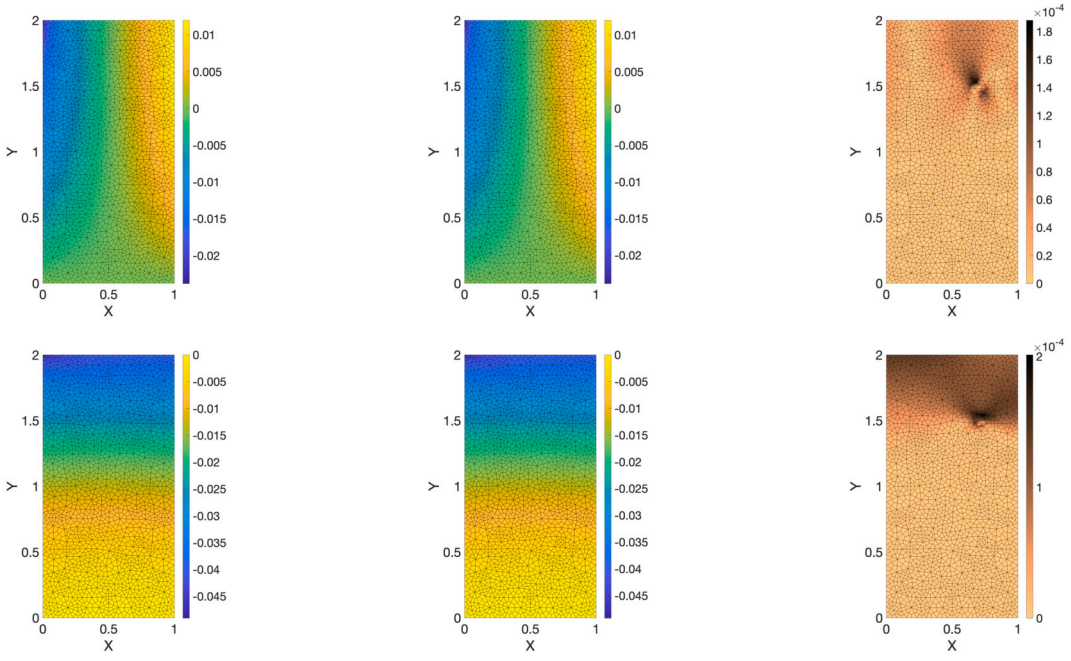

Fig. 4. x (**top**), y (**bottom**) components of the displacement field associated with the nominal solution (**left**); reference solution that takes into account the real damaged region (**middle**) and difference in absolute between the two solutions (**right**) at time $t = 7.24$ s.

4.3. Cantilever

In this section, we consider a cantilever fully clamped on its left side, free on the other boundaries and subjected to a vertical load on its right side bottom corner. The force (Fig. 10b) applied to the structure is:

$$f(t) = -10^7 \cdot \left(2\pi^2 \frac{(t-5)^2}{25} - 1\right) \cdot e^{\left(-\pi^2 \frac{(t-5)^2}{25} - 1\right)} \cdot sin(6\pi \cdot t). \tag{18}$$

The structure is modeled under a plane stress condition and its behavior is assumed to be elastic, characterized by a Young's modulus of $E = 200$ GPa and a Poisson's coefficient of $\nu = 0.3$. This configuration corresponds to the nominal structural system, while the reference system is assumed to contain a damaged area. The structure is equipped with a finite element mesh (Fig. 10a), where the elements located in the damaged region are highlighted in red. In this region, the Young's modulus is reduced to $E' = 0.2 \cdot E$. For this case due to computational burden only two frequencies have been chosen (33, 150 Hz) to run the algorithm (15). Fig. 11 compare the displacement field (x and y components) of the damaged and undamaged structures at 5.42 seconds. The results of the identification procedure are displayed in Fig. 12, il-

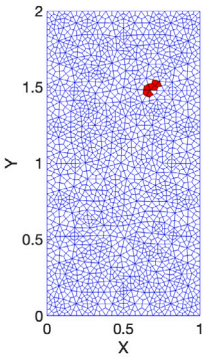

(a) Elements identified (in red) at the first iteration (q=1) of the algorithm. These elements are those whose stiffness mostly differs from the nominal one.

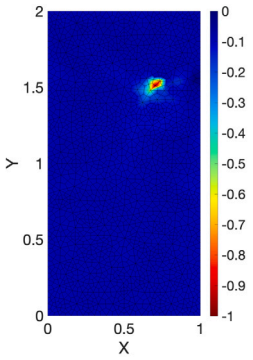

(b) Coefficients a_i in the entire structure representing the identification of the damage and the correction of the model.

Fig. 5. Result of the identification.

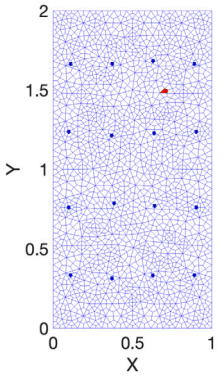

(a) Damaged element (red) and sensor distribution (blue nodes).

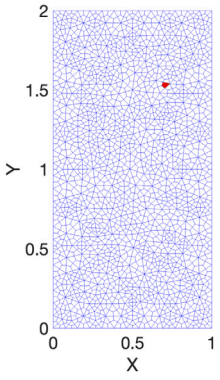

(b) Elements identified, as the most probable to be damaged.

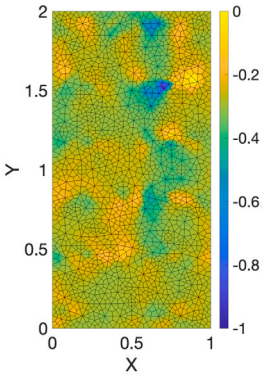

(c) Coefficients a_i in the entire structure.

Fig. 6. Result of the identification when only one element is damaged.

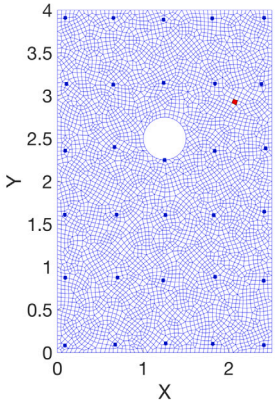

(a) Damaged region (red element) in the plate with an hole and location of the 30 sensors (blue nodes).

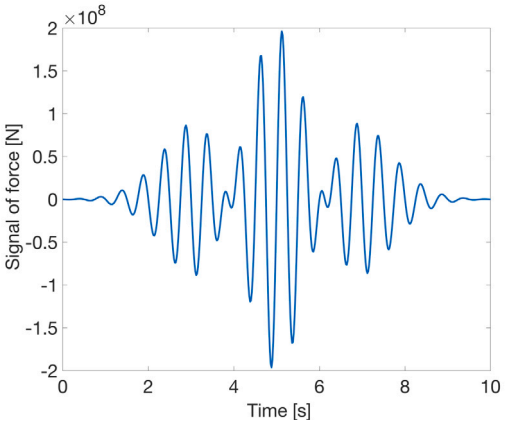

(b) Magnitude of the load over time ($f(t)$) applied to the plate with an hole. The load has the same component in the x and y directions.

Fig. 7. Problem configuration plate with hole.

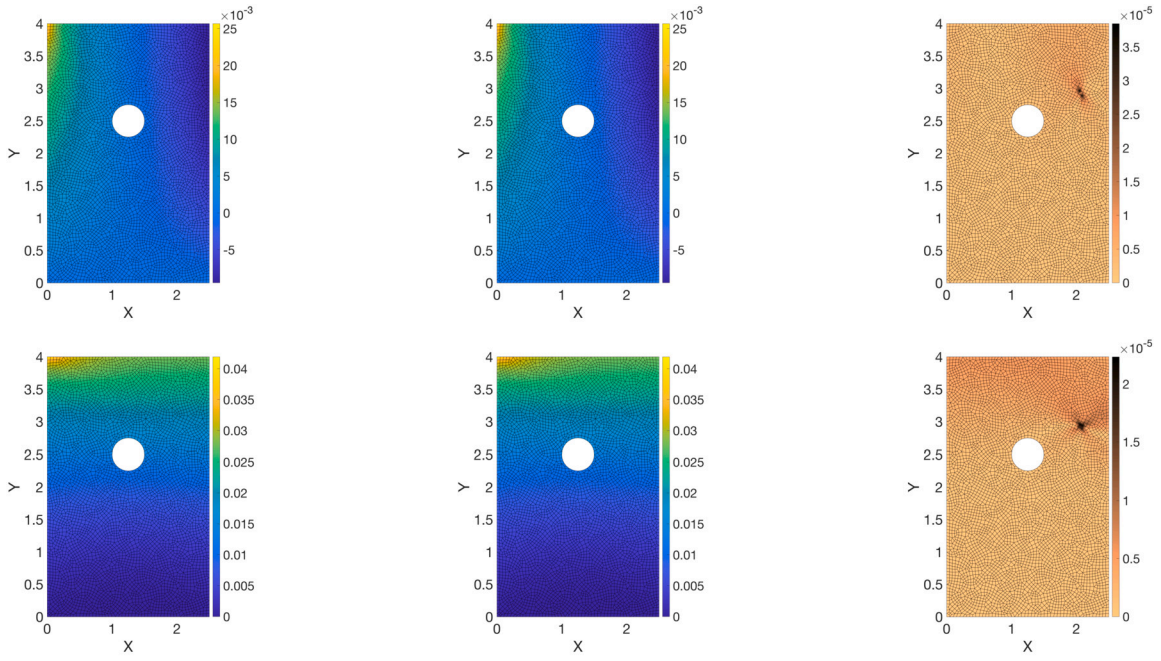

Fig. 8. x (**top**), y (**bottom**) components of the displacement field associated with the nominal solution (**left**); reference solution that takes into account the real damaged region (**middle**) and difference in absolute between the two solutions (**right**) at time $t = 5.12$ s.

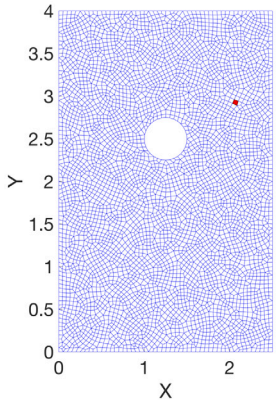

(a) Element identified (in red) at the first iteration (q=1) of the algorithm as damage.

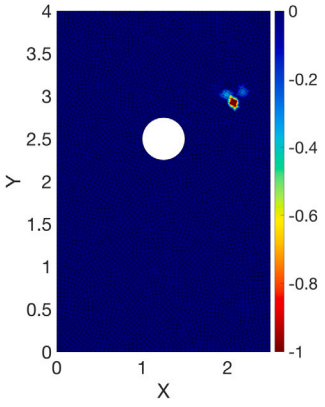

(b) Coefficients a_i in the entire structure representing the identification of the damage.

Fig. 9. Result of the identification on the plate with an hole.

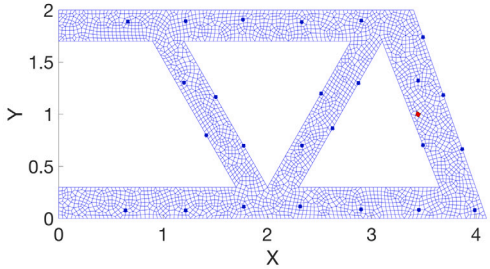

(a) Damaged region (red element) in the structure and location of the 25 sensors (blue nodes).

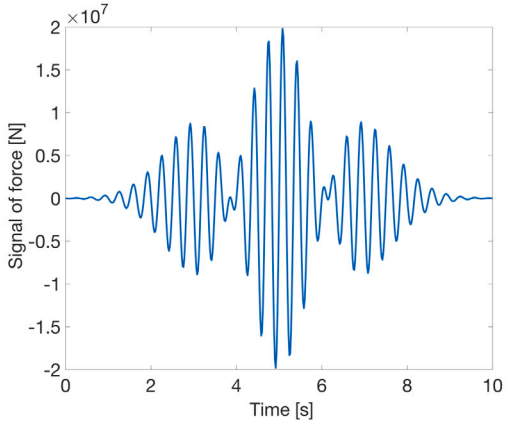

(b) Magnitude of the load over time ($f(t)$) applied to the cantilever. The load has only a y component.

Fig. 10. Problem configuration cantilever.

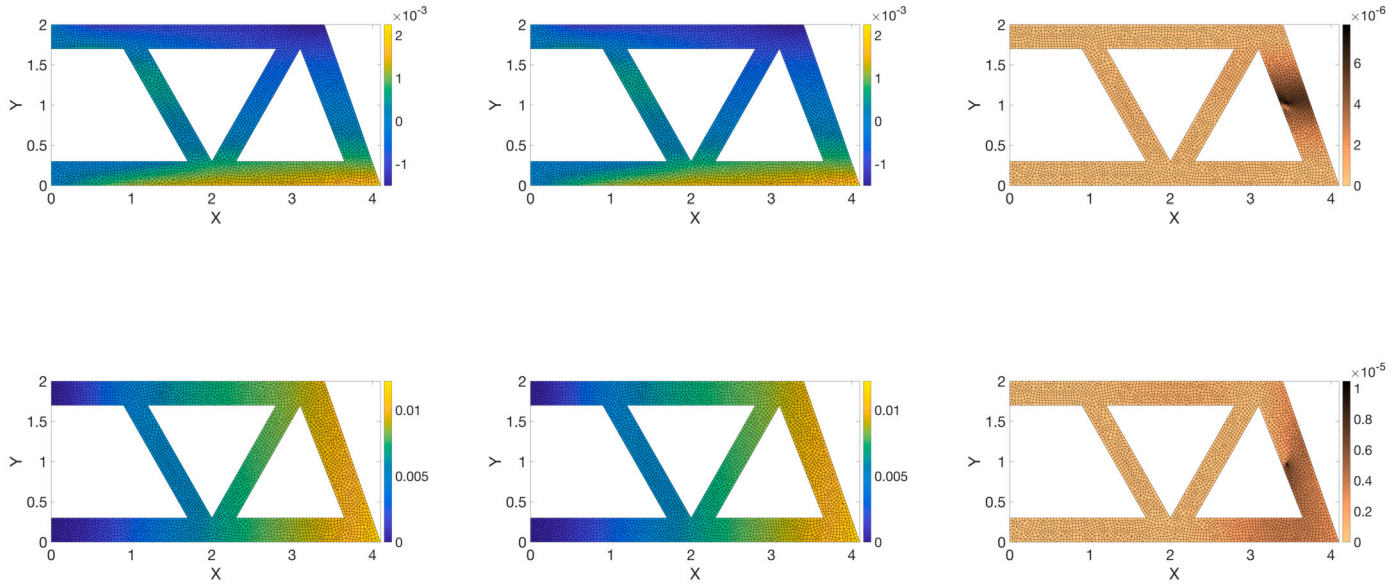

Fig. 11. x (**top**), y (**bottom**) components of the displacement field associated with the nominal solution (**left**); reference solution that takes into account the real damaged region (**middle**) and difference in absolute between the two solutions (**right**) at time $t = 5.42$ s.

(a) Element identified (in red) at the first iteration (q=1) of the algorithm as damage.

(b) Coefficients a_i in the entire structure representing the identification of the damage.

Fig. 12. Result of the identification on the cantilever.

lustrating that the algorithm accurately identifies the location of the damage. The prediction of damage localization in the numerical examples presented in the last sections is mainly achieved due to the L1 regularization on the a-coefficients, which induces the model enrichments to be very localized. The above property is reinforced by the fact that the model determines the best local enrichment such that it can better correct the frequency response of the experimentally measured displacement, which makes the method even more robust.

5. Conclusions and perspectives

A local material enrichment algorithm for the identification of structure damage has been proposed. This method is robust in identifying very localized damage despite being applied to very rigid structures in the presence of few sensors, moreover, the method achieves damage localization even if the sensors are far away from the damaged area, which demonstrates the capabilities of the proposed method.

Since the present work focuses its attention mainly on the development of ideas, its application is kept here for academic examples. Thus, extensions should be carried out to be applied to realistic cases and to bring its application closer to the industrial world. In this sense, progress continues to be made in the direction of enriching the physical model with more complex behaviors, in order to be able to identify corrections in the model that take into account more complex phenomena, such as anisotropic or nonlinear behavior. Another perspective to be mentioned corresponds to the extension of the method in the case that the experimental measurements do not correspond to displacements, but rather to strains, and that these do not contain the measurement of all the components of the strain tensor. The above perspectives, both for the enrichment of the method for local correction taking into account complex behaviors, as well as the extension of the methodology for incomplete deformation tensor measurements, are considered as crucial to provide the method with the capability to be widely used in an industrial context. These developments will be presented in future publications.

CRediT authorship contribution statement

D. Di Lorenzo: Writing – review & editing, Writing – original draft, Visualization, Project administration, Methodology, Investigation, Conceptualization. **S. Rodriguez:** Writing – review & editing, Investigation, Validation, Data curation, Writing – original draft. **V. Champaney:** Conceptualization, Validation, Writing – original draft, Investigation. **C. Germoso:** Supervision, Writing – review & editing, Data curation. **M. Beringhier:** Validation, Supervision, Investigation. **F. Chinesta:** Conceptualization, Methodology, Supervision.

Declaration of competing interest

The authors declare that they have no known competing financial interests or personal relationships that could have appeared to influence the work reported in this paper.

Data availability

Data will be made available on request.

Acknowledgements

We acknowledge the financial support from the European Union Horizon 2020 research and innovation program under the Marie Skłodowska-Curie grant agreement No. 956401 (XS-Meta).

References

[1] N.F. Alkayem, M. Cao, Y. Zhang, M. Bayat, Z. Su, Structural damage detection using finite element model updating with evolutionary algorithms: a survey, Neural Comput. Appl. 30 (2018) 389–411.

[2] N. Maia, J. Silva, R. Sampaio, Localization of damage using curvature of the frequency-response-functions, in: Proceedings of the 15th International Modal Analysis Conference, vol. 3089, 1997, p. 942.

[3] X. Liu, N. Lieven, P.J. Escamilla-Ambrosio, Frequency response function shape-based methods for structural damage localisation, Mech. Syst. Signal Process. 23 (4) (2009) 1243–1259.

[4] S. Rucevskis, R. Janeliukstis, P. Akishin, A. Chate, Mode shape-based damage detection in plate structure without baseline data, Struct. Control Health Monit. 23 (9) (2016) 1180–1193.

[5] G. Sha, M. Radzieński, M. Cao, W. Ostachowicz, A novel method for single and multiple damage detection in beams using relative natural frequency changes, Mech. Syst. Signal Process. 132 (2019) 335–352.

[6] S.R. Ibrahim, E. Mikulcik, A method for the direct identification of vibration parameters from the free response, in: The Shock and Vibration Inform. Ctr. Shock and Vibration Bull. Part. 4: Sep. 1977, 1977.

[7] J.K. Vandiver, A.B. Dunwoody, R.B. Campbell, M.F. Cook, A mathematical basis for the random decrement vibration signature analysis technique, J. Mech. Des. 104 (2) (1982) 307–313, https://doi.org/10.1115/1.3256341.

[8] J.-N. Juang, R.S. Pappa, An eigensystem realization algorithm for modal parameter identification and model reduction, J. Guid. Control Dyn. 8 (5) (1985) 620–627.

[9] S.R. Ibrahim, Double least squares approach for use in structural modal identification, AIAA J. 24 (3) (1986) 499–503.

[10] J. Cattarius, D. Inman, Time domain analysis for damage detection in smart structures, Mech. Syst. Signal Process. 11 (3) (1997) 409–423.

[11] B. Peeters, G. De Roeck, Stochastic system identification for operational modal analysis: a review, J. Dyn. Syst. Meas. Control 123 (4) (2001) 659–667.

[12] B. Xu, V. Giurgiutiu, L. Yu, Lamb Waves Decomposition and Mode Identification Using Matching Pursuit Method, Sensors and Smart Structures Technologies for Civil, Mechanical, and Aerospace Systems 2009, vol. 7292, SPIE, 2009, pp. 161–172.

[13] A. Raghavan, C.E. Cesnik, Guided-wave signal processing using chirplet matching pursuits and mode correlation for structural health monitoring, Smart Mater. Struct. 16 (2) (2007) 355.

[14] Y. Lu, J.E. Michaels, Numerical implementation of matching pursuit for the analysis of complex ultrasonic signals, IEEE Trans. Ultrason. Ferroelectr. Freq. Control 55 (1) (2008) 173–182.

[15] W. Mu, Y. Gao, G. Liu, Ultrasound defect localization in shell structures with lamb waves using spare sensor array and orthogonal matching pursuit decomposition, Sensors 21 (23) (2021) 8127.

[16] Z. Su, L. Ye, Y. Lu, Guided Lamb waves for identification of damage in composite structures: a review, J. Sound Vib. 295 (3–5) (2006) 753–780, https://doi.org/10.1016/j.jsv.2006.01.020.

[17] Z. Su, L. Ye, Identification of Damage Using Lamb Waves, Lecture Notes in Applied and Computational Mechanics, vol. 48, Springer, London, 2009.

[18] M. Mitra, S. Gopalakrishnan, Guided wave based structural health monitoring: a review, Smart Mater. Struct. 25 (5) (2016) 053001, https://doi.org/10.1088/0964-1726/25/5/053001, https://iopscience.iop.org/article/10.1088/0964-1726/25/5/053001.

[19] X. Qing, W. Li, Y. Wang, H. Sun, Piezoelectric transducer-based structural health monitoring for aircraft applications, Sensors 19 (3) (2019) 545, https://doi.org/10.3390/s19030545, http://www.mdpi.com/1424-8220/19/3/545.

[20] C.-C. Chang, L.-W. Chen, Damage detection of a rectangular plate by spatial wavelet based approach, Appl. Acoust. 65 (8) (2004) 819–832.

[21] H. Kim, H. Melhem, Damage detection of structures by wavelet analysis, Eng. Struct. 26 (3) (2004) 347–362.

[22] M. Rucka, K. Wilde, Application of continuous wavelet transform in vibration based damage detection method for beams and plates, J. Sound Vib. 297 (3–5) (2006) 536–550.

[23] W. Fan, P. Qiao, A 2-d continuous wavelet transform of mode shape data for damage detection of plate structures, Int. J. Solids Struct. 46 (25–26) (2009) 4379–4395.

[24] Y. Huang, D. Meyer, S. Nemat-Nasser, Damage detection with spatially distributed 2d continuous wavelet transform, Mech. Mater. 41 (10) (2009) 1096–1107.

[25] D. Di Lorenzo, V. Champaney, C. Germoso, E. Cueto, F. Chinesta, Data completion, model correction and enrichment based on sparse identification and data assimilation, Appl. Sci. 12 (15) (2022).

[26] O.C. Zienkiewicz, R.L. Taylor, The Finite Element Method for Solid and Structural Mechanics, Elsevier, 2005.

[27] M. Grant, S. Boyd, Graph implementations for nonsmooth convex programs, in: V. Blondel, S. Boyd, H. Kimura (Eds.), Recent Advances in Learning and Control, Lecture Notes in Control and Information Sciences, Springer-Verlag, Limited, 2008, pp. 95–110, http://stanford.edu/~boyd/graph_dcp.html.

[28] M. Grant, S. Boyd, CVX: Matlab software for disciplined convex programming, version 2.1, https://cvxr.com/cvx, Mar. 2014.